Method for including electron-electron collisions in Monte Carlo simulations of electron swarms in partially ionized gases

Yilin Weng and Mark J. Kushner

Department of Electrical and Computer Engineering, University of Illinois,
1406 West Green Street, Urbana, Illinois 61801
(Received 6 June 1990)

A method whereby electron-electron collisions can be included in Monte Carlo simulations of electron swarms in low-temperature partially ionized plasmas is presented. In this method, electron-electron (e-e) collisions are treated as being functionally equivalent to electron–neutral-species collisions. In doing so, individual pseudoelectron particles in the simulation collide with an energy-resolved electron fluid. Energy is exchanged with this fluid using the Coulomb cross section. When e-e collisions dominate, the electron-energy distribution evolves to being Maxwellian. The method is made computationally tractable by using a modified null-cross-section technique that eliminates the need for recalculating collision probabilities as the electron-energy distribution evolves.

I. INTRODUCTION

The use of particle simulations to calculate electron-transport coefficients and electron-energy distributions (EED's) in fully and partially ionized plasmas is a well-established technique.[1-8] Particle simulations are particularly useful for modeling electron transport when the EED is not in equilibrium with the local electric field (either temporally or spatially), or when complex geometries are considered. In this respect, particle simulations of low-temperature partially ionized plasmas ($10^{-6} \leq n_e/N \leq 10^{-1}$, $0.1 \leq T_e \leq 10$ eV) have been used to model electron transport in the cathode falls of glow discharges, radio-frequency (rf) plasmas, and pulse power switches.[9-16]

Low-temperature partially ionized plasmas (LTPIP's), as used for plasma-assisted material processing, lasers, and plasma switches, differ from fully ionized plasmas in that electron transport is usually dominated by collisions with neutral atoms and molecules. As the fractional ionization significantly exceeds 10^{-4}, though, electron-electron (e-e) collisions begin to have an important impact on the EED. In the limit that e-e collisions dominate, the EED evolves towards being Maxwellian. Partially ionized plasmas having these characteristics include electron cyclotron resonance (ECR) excited discharges[17-19] and magnetron devices,[20,21] both of which are currently being developed for use in plasma etching and deposition of semiconductor materials. The fractional ionization of ECR plasmas as used for remote plasma-activated chemical-vapor deposition (RPACVD) are in the range of 5×10^{-5}– 2×10^{-3} with total gas pressures of 10^{-5}–10^{-2} Torr. Cylindrical rf magnetron discharges used for etching of semiconductors also have fractional ionizations as high as 2×10^{-3} and total gas pressures of 5×10^{-4}–5×10^{-3} Torr. Particle simulations of LTPIP's using Monte Carlo methods, though, do not typically include e-e collisions. This exclusion limits the class of plasmas for which these particle simulations may be used, particularly those devices described above. Particle-in-cell simulations (PICS) are now being used to model LTPIP's,[13,16] and these simulations do, to some degree, include e-e collisions. For the reasons discussed below, however, traditional PICS are computationally intensive. One is therefore motivated to develop other particle techniques to model the plasmas of interest.

In this paper, we present a method whereby e-e collisions may be included in a Monte Carlo simulation of electron swarms in LTPIP's where inelastic collisions with neutral species dominate the loss of energy by electrons. In this method, collisions of electrons with electrons are conceptually treated the same way as collisions of electrons with heavy particles (atoms and molecules). This is accomplished by having the electron particles in the simulation collide with an energy-resolved electron fluid in the same manner that electrons collide with the neutral heavy-particle fluid. In doing so, the impact-Lorentz approximation may be used for the collisions of electron particles with the electron fluid. The advantages of this method are that the same algorithms are used for all collisions, and the integrating time step may be as large as the time between collisions. To make this technique computationally tractable, a modified null-cross-section algorithm is employed which eliminates the need for recomputing the probability integrals for electron collisions as the EED evolves.[22] The method can have a response time of $\leq$ tens of nanoseconds, thereby enabling one to simulate transient phenomena having tens of megahertz frequency. In Sec. II, we discuss the motivation for developing this new method and in Sec. III, our method is described in detail. The technique is demonstrated in Sec. IV, where electron-energy distributions are presented for swarms in N_2 and Ar, and plasma-processing reactors.

II. THE APPLICATION OF PARTICLE SIMULATIONS TO MODELING PARTIALLY IONIZED PLASMAS

Particle simulations of plasmas may be divided into two generic categories: particle in cell simulations (PICS) and Monte Carlo simulations (MCS). The two methods employ many of the same techniques to advance particle trajectories and to solve Poisson's equation for changes in the electric field. In this paper, we differentiate between PICS and MCS by the manner in which collisions are modeled. In this respect, PICS are most commonly applied to the simulation of fully ionized plasmas.[4] In a PICS, the equations of motion of electrons and ions are integrated while including both external and interparticle forces. Perturbations to the trajectories of particles resulting from interparticle forces constitute collisions. These interparticle forces often determine the size of the time and spatial steps which may be used to advance the particles. Since in a fully ionized plasma the interparticle forces are Coulombic, collisions are long range (hundreds of angstroms). Typically, there are no short-range (a few angstroms) forces which result in inelastic energy losses, as there are during electron–neutral-species (e-N) collisions in LTPIP's. The Coulomb forces between charged particles may be included in the simulation in one of two ways. The first is by explicitly summing the interparticle forces and adding the net force to that given by the applied electric or magnetic field,

$$\mathbf{F}_i = -e\left[\mathbf{E} + \mathbf{v}\times\mathbf{B} + \sum_j \frac{(\pm e^2)}{|\mathbf{r}_j - \mathbf{r}_i|^2}(\mathbf{r}_j - \mathbf{r}_i)\right], \qquad (1)$$

where the sum is over electrons and ions in the plasma, and $\mathbf{E}$ and $\mathbf{B}$ are the applied vacuum fields. This method is called a particle-particle (PP) technique,[1] and is functionally equivalent to solving the Fokker-Planck equation.

In the second method, Coulomb forces on electrons are obtained by explicitly including the electron and ion charges in solution of Poisson's equation. This is accomplished by summing the electron and ion densities on a computational mesh to obtain the charge density, which is then used in solving Poisson's equation. The resulting electric field has the spatial resolution of the mesh. This method is known as a particle-mesh (PM) technique,[1] and is functionally equivalent to solving Vlasov's equation.

To resolve the interparticle forces using either PP or PM techniques, the spatial resolution should be on the order of the Debye length and there must be many electrons in a Debye sphere. In typical high-temperature fully ionized plasmas, the electron temperature and density are approximately $T_e \approx 20$ keV and $n_e \approx 10^{13}$ cm^{-3}. The resulting Debye length and number of electrons in a Debye sphere are $\lambda_D \approx 0.035$ cm and $n_D \approx 2 \times 10^8$. [Each pseudoparticle in the simulation may, of course, represent many actual electrons (e.g., 10^5–10^9).] In a LTPIP, as used for plasma etching, $T_e \approx 2$ eV and $n_e \approx 10^9$ cm^{-3}. This results in a similar value for λ_D (≈ 0.03 cm) and a smaller value of n_D ($\approx 2 \times 10^5$). The computational spatial mesh in each case must therefore be very fine ($\ll$ millimeters), the integration step quite small ($\ll$ picoseconds), and the number of computational particles large. These requirements may be somewhat relaxed by using numerical averaging techniques. One such method is to use finite-sized particles (FSP) where the charge density of individual computational particles is averaged over adjacent mesh points.[3] This technique, however, also smoothes the small changes in charge density, and hence interparticle forces, which constitute an e-e collision. Therefore when e-e collisions compete with inelastic electron–neutral-species collisions, as in a partially ionized plasma, there may be a systematic biasing of the relative amount of energy which is exchanged in e-e collision as compared to that exchanged in e-N collisions.

In a LTPIP, momentum-transfer collisions and inelastic collisions with heavy neutral particles (atoms and molecules) are usually most important in determining the EED, and hence in determining electron-transport coefficients. These collisions result from short-range forces having spatial extents of angstroms. Since the electron thermal velocity is typically $> 10^7$ cm s^{-1}, the durations of e-N collisions are $< 10^{-15}$ s. In addition, the temperature of the neutral heavy particles is 10^{-1}–10^{-3} that of the electrons, resulting in heavy-particle thermal velocities which are 10^{-2}–10^{-4} that of the electrons. Because of these conditions, e-N collisions are most often simulated using the impact-Lorentz approximation. This approximation states that collisions between electrons and heavy neutral particles occur over a time period (10^{-15} s) and distance (10^{-8} cm) which are insignificantly small compared to other time and spatial scales, such as the Debye length (less than tens of micrometers) and the time between collisions. (The time between collisions scales as 1 ns/p, where p is the gas pressure in Torr.) Therefore, one approximates that e-N collisions occur instantaneously, without change in the spatial location of the electron, and that the relative motion of the heavy particle is not important in computing the collision integral. The use of these approximations, and the method of determining when a collision takes place, differentiate a MCS from a PICS. Therefore, a MCS is the more appropriate vehicle for calculating the EED of a LTPIP.

The dynamics *during* a collision are not resolved in a MCS. The important collision parameters are the time between collisions, and which particular collision (e.g., elastic, vibrational excitation, ionization) occurs in each instance. These decisions are made by choosing a sequence of random numbers, as described in Sec. III. When a particular collision has been selected, the energy and trajectory of the electron having had the collision are instantaneously changed in accordance with the energy loss and differential scattering cross section. Therefore the trajectory of the particle may, in principle, be advanced using time increments as large as the time between collisions, unless constrained by other processes such as local variations in the electric field.

There are number of computational difficulties encountered in attempting to include e-e collisions in a MCS of a LTPIP. The first difficulty is that even though the frequency of e-e collisions may be small compared to e-N

collisions, the rate of energy exchange may be high compared to e-N collisions. This condition results from the fact that in an e-e collision, the collision partners may completely exchange their energy. In e-N "elastic" collisions, the fractional energy exchange is limited to $2m_e/M$. Therefore, energy exchange may be significantly altered by relatively infrequent e-e collisions. This condition requires a large number of particles to statistically resolve the interaction. A second problem, described above, is that the spatial scales of e-e and e-N collisions are dramatically different. Using either PP or PM methods to include e-e collisions in a MCS requires a resolution much less than λ_D, which is typically much smaller than the distance between collisions ($0.3/p$ cm). Time steps much smaller than the time between collisions must also be used. If a PM method is used, smoothing algorithms may be applied, such as the FSP, to lessen this requirement. It is well known, though, that LTPIP's are quasineutral (e.g., $\nabla \cdot \mathbf{E} \simeq 0$) over macroscopic distances (millimeters to centimeters) outside of sheaths. Therefore numerical techniques which require one to resolve spatial scales at all times which are significantly less than that dictated by quasineutrality are inefficient. Also, methods which require one to use different algorithms for e-e and e-N collisions due to their different spatial scales will also be inefficient. We are, then, motivated to treat e-e collisions in a similar fashion to e-N collisions to avert these problems.

III. DESCRIPTION OF THE MODEL

The goal of our method for modeling e-e collisions in MCS of LTPIP's is to include those collisions in a manner which is functionally the same as e-N collisions. By meeting this goal, the impact approximation may be used, the spatial resolution of the calculation is not limited to λ_D, and quasineutrality may be invoked. Before describing our model, we will briefly review our implementation of the Monte Carlo method and the use of the null cross section.

A. The Monte Carlo method using null collisions

Prior to beginning the MCS, a gas mixture is selected and the energy range of interest is divided into bins centered at ε_i. The total electron collision frequency in each energy interval ν_i is determined and probability arrays are initialized for each energy interval. The probability arrays are denoted P_{ij} for energy i and collision process j. They have the properties that

$$P_{i,j} = \frac{\nu'_{i,j}}{\nu_i}, \quad \nu'_{i,j} = \sum_{l=1,j} \nu_{i,l} , \tag{2}$$

where $\nu_{i,j}$ is the collision frequency for energy interval i and process j, $\nu'_{i,j}$ is the cumulative collision frequency for processes $l \leq j$, and $P_{i,j}$ is normalized so that for m processes, $P_{i,m} = 1$. The difference between elements of $P_{i,j}$ represent the relative probability of an electron undergoing a particular collision at a specific energy.

The trajectory of an electron having energy ε_i moving in a uniform electric field may be updated using average time steps of $1/\nu_i$ if the impact approximation is used, since during this time the electron is accelerated by only the electric field. Using the Monte Carlo method, the actual time step for advancing a particular particle is obtained from $\Delta t = -\ln(r_1)/\nu_i$, where r_1 is the first in a sequence of random numbers which are uniformly distributed on (0,1). Given this time step, the position and velocity of the electron are updated by integrating the equations of motion for Δt. At the end of this update, a collision occurs. The type of collision that occurs is obtained by choosing a second random number r_2. The collision, denoted j, is that process which satisfies

$$P_{i,j-1} < r_2 \leq P_{i,j} . \tag{3}$$

The energy of the electron is revised to $\varepsilon \rightarrow \varepsilon - \Delta \varepsilon_{i,j}$, where $\Delta \varepsilon_{i,j}$ is the change in energy (loss for inelastic, gain for superelastic) associated with process j at energy i. The velocity of the electron is updated based on the change in energy and the scattering angle given by the differential cross section.

If the acceleration of the electron during its flight between collisions significantly changes its energy, its total collision frequency may also change. In this case, the choice of Δt is ambiguous because ν_i at the beginning of the flight differs from that at the end of the flight. This complication may be avoided by using a null cross section[22] or "self-scattering" event.[23] In this method, the maximum electron collision frequency, ν_m, over the energy interval of interest is determined. An additional fictitious or "null" collision process is added to the real processes at each energy. The null collision process at energy ε_i has collision frequency $\nu_{in} = \nu_m - \nu_i$. In doing so, the time between collisions for electrons at all energies can unambiguously be given by $\Delta t = -\ln(r_i)/\nu_m$. After updating the velocity and location of the particle using this time step, another random number is chosen. If $r_2 > \nu_{in}/\nu_m$, where the energy bin i is based on the instantaneous energy of the electron, then a real collision has occurred, and the particle's velocity is revised accordingly. The specific collision which occurs is obtained by using r_2 to search the probability arrays as shown in Eq. (3). If, however, $r_2 \leq \nu_{in}/\nu_m$, then a "null" collision occurs and the particle proceeds to its next "collision" unhindered.

B. The equivalence method for including electron-electron collisions

The basis of our method to include e-e collisions in MCS is to treat e-e collisions functionally the same as e-N collisions. That is, instead of having electrons collide with individual electrons, as in a PP technique, the electrons collide with an energy-resolved electron fluid in the same manner as electrons collide with the neutral fluid. The implementation then resembles a PM technique. In doing so, we must implicitly assume that changes in charge densities which may occur on spatial scales of $\ll \lambda_D$ are not a result of, or do not contribute to, Coulomb collisions between electrons. In the bulk plas-

ma, where quasineutrality holds over dimensions much greater than λ_D, this is a good approximation for the plasmas of interest. The change in electric field which results from there being a finite charge density in, for example, the sheath regions may be included in this method with no change in the algorithm. The charge density used in Poisson's equation under these conditions must be calculated using a coarse spatial filter (e.g., FSP smoothing). This filtering is required so that small fluctuations in the charge density which generate the electric field constituting the e-e collision do not feed back to the simulation, thereby double counting the effects of the collisions.

In e-N collisions the distribution of heavy-particle velocities is usually unimportant in calculating the collision frequency or energy loss. In e-e collisions, both the collision frequency and energy loss are quite sensitive to the relative velocities of the incident and target electrons, which in this case are the relative velocities of the electron particle and the velocity distribution of the electron fluid. To accommodate these dependencies, the electron fluid is divided into velocity classes, or "bins." Each velocity class of the electron fluid is functionally treated as a separate species in the model. Therefore, e-e collisions are included by having the incident electron particles collide with an ensemble of electron fluids, each having a fixed velocity, and each being treated equivalently to the background neutral fluid.

For example, let the collision cross section for process j between an electron having velocity $\mathbf{v}$ and collision partner having velocity $\mathbf{u}$ be $\sigma_j(\mathbf{v},\mathbf{u})$. If the velocity distribution of the collision partner is $f(\mathbf{u})$, then the electron-collision frequency for the process ν_j is

$$\nu_j(\mathbf{v}) = N \int |\mathbf{v}-\mathbf{u}'|\sigma_j(\mathbf{v},\mathbf{u}')f(\mathbf{u}')d^3\mathbf{u}' , \qquad (4)$$

where N is the number density of the collision partner. If the collision is with a heavy particle and the impact-Lorentz approximation is valid, then we can approximate that $\nu_j(v) \approx N\bar{\sigma}_j(v)$, where $\bar{\sigma}_j(v) = \int \sigma_j(\mathbf{v},\mathbf{u}')f(\mathbf{u}')d^3\mathbf{u}$ is the electron impact cross section averaged over the velocity distribution of the heavy particles. In doing so, we assume that $f(\mathbf{u})$ for the heavy particles is known, as in the Lorentz approximation, or is implicitly included in the measurement of $\bar{\sigma}_j(v)$. This approximation cannot be made in the case of e-e collisions because the integral in Eq. (4) acutely depends on the velocity distribution of the target electrons, which in this case is the velocity distribution of the electron fluid.

In order to treat e-e collisions the same as e-N collisions by specifying a collision frequency for the process, one must be able to calculate the frequency of e-e collisions as a function of the relative velocity between the incident electrons and the electron fluid. This frequency may be obtained from Eq. (4) by using the velocity distribution of the electron fluid $f_e(\mathbf{u})$, the Coulomb cross section $\sigma_{e-e}(\mathbf{v},\mathbf{u})$, and the electron density n_e. The frequency is

$$\nu_{e-e}(\mathbf{v}) = n_e \int |\mathbf{v}-\mathbf{u}'|\sigma_{e-e}(\mathbf{v},\mathbf{u}')f_e(\mathbf{u}')d^3\mathbf{u} . \qquad (5)$$

Using discrete electron bins, Eq. (5) is rewritten as

$$\nu_{ee}^i = \sum_j \nu_{e-e}^{ij} = n_e \sum_j \nu_{ij}\sigma_{e-e}(\nu_{ij})f_j\Delta\varepsilon_j . \qquad (6)$$

In Eq. (6), ν_{e-e}^i is the e-e collision frequency for particle electrons having energies in the interval $(\varepsilon_i, \varepsilon_i + \Delta\varepsilon_i)$, ν_{e-e}^{ij} is the e-e collision frequency between incident electrons in energy interval i and the electron fluid in energy interval j, ν_{ij} is the interaction speed between incident electrons and fluid electrons in energy intervals i and j, and σ_{e-e} is the interaction cross section. The fraction of fluid electrons per unit energy in interval j is f_j having normalization $\sum_j f_j \Delta\varepsilon_j = 1$. In writing Eq. (6), we are expressing the rate of e-e collisions for an electron in energy interval i as the sum of collision frequencies with discrete portions of the electron fluid distribution. In doing so, each energy interval of the electron fluid is treated *exactly as we would an atomic species having density* $n_e f_j \Delta\varepsilon_j$. That is, in calculating ν_i, we add the contributions of the ν_{e-e}^{ij} to the frequencies for the e-N collisions just as though they were heavy-particle collisions. By choosing random numbers as described above, we obtain a distribution of e-e collisions weighted in correct proportion to those for e-N collisions. By characterizing the electron fluid in terms of energy, though, the vector information required to solve the collision integral in Eq. (5) is lost.

The formulation presented above appears ill posed since we require prior knowledge of $f_e(\mathbf{u})$ in the form of f_j to obtain the EED, which for a self-consistent solution should be mirrored by $f_e(\mathbf{u})$. In our model the values of f_j are obtained during the simulation by sampling the EED of the particles and updating f_j as the EED evolves. This process is performed by using a modified null-cross-section technique. The method eliminates the need to recompute the probability array as the EED evolves, and therefore is computationally efficient. This implementation is described below.

C. Modified null-cross-section technique

The simulation begins by calculating the probability arrays [Eq. (2)] using collision frequencies ν_{ij}. When modeling e-e collisions, the collision frequencies ν_{e-e}^{ij} are included in this calculation. The electron fluid elements are then represented in the array as a separate species having densities $n_e f_j \Delta\varepsilon_j$. The values of ν_{e-e}^{ij} are initially obtained using a trial electron-energy-distribution function for the f_j and applying Eq. (6). In the usual method the probability of having null collisions is included in the arrays by searching for the maximum collision frequency ν_m, and adding $\nu_{in} = \nu_m - \nu_i$ to the real collision frequencies. The modified null-cross-section technique involves using an additional null-collision frequency, ν_{in}^{e-e}, when calculating the probability arrays. The additional null-collision probability is conceptually allocated to the space for e-e collisions, as shown in Fig. 1. The probability allocated to e-e collisions therefore contains space temporarily allocated to real collisions and to null collisions. The precise values of the ν_{in}^{e-e} are not critical. They only need to be larger than the maximum value of ν_{e-e}^i which one might encounter during the simulation as the EED evolves.[24]
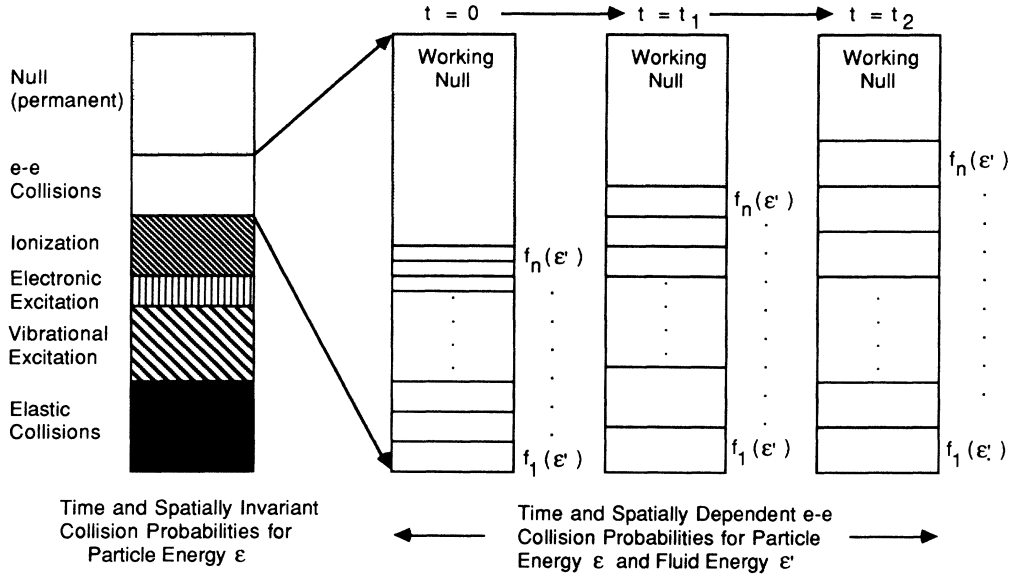
FIG. 1. Schematic of the hierarchy of collision probabilities and the division between real and null collision frequencies used in the model. The column at left represents the relative probability of electron collisions at a specific energy. The probability may include a portion which is permanently allocated to null collisions. The portion allocated to *e-e* collisions is divided into real collisions and a working null area. As the electron-energy distribution evolves, either spatially or temporally, the space allocated to real *e-e* collisions expands or contracts at the expense of the working null space.

The calculation then proceeds as follows. A sequence of random numbers is chosen as described above. The random numbers are used to advance the electron particles, to determine if the collision is real or null, and to choose the type of collision which occurs (see Fig. 1). If the sequence results in choosing an *e-e* collision, an additional random number is chosen to determine if the *e-e* collision is itself real or null. As the simulation proceeds and the EED evolves, the values of v_{e-e}^{ij} are periodically updated based on a sampling of the instantaneous distribution function. In this manner, self-consistency is obtained. By having previously allocated "working" null space in the original probability arrays, the values of v_{e-e}^{ij} do not need to be actually recalculated. The update only requires one to take a ratio between the current value of f_j and that value which was used to construct the original probability array. The real *e-e* collision probability then expands and contracts, at the expense of space allocated for null collisions, as the simulation progresses. Using this method, the probabilities for *e-N* collisions do not have to be recalculated either. In practice, we have found that the EED equilibrates with only a few updates of the probability arrays. For example, in simulating an electron swarm in N_2 with $E/N = 20 \times 10^{-17}$ V cm^2 and with $n_e/N = 5 \times 10^{-4}$, the distribution function equilibrates in only a few tens of ns when using a few hundred particles. We therefore may perform time-dependent calculations with frequencies exceeding a few tens of megahertz using this technique.

By using the modified null-cross-section technique, the extension of our method to multiple spatial dimensions is straightforward. This is accomplished by collecting

statistics as a function of position during the simulation to obtain intermediate values of $f_j(\mathbf{x})$. Those values are then used to scale the probability for *e-e* collisions between real and null processes as a function of position. This treatment effectively treats the electron fluid velocity elements at different spatial points as separate species with which the incident electrons can collide. Again, only a single probability array is required which has adequate working null space to accomodate differences in the rate of *e-e* collision as a function of position. A changing electron density can also be accounted for in this manner by including enough working null space to cover any increase in the rate of *e-e* collisions resulting from the increase in electron density. One pays the penalty, though, that the number of null collisions will increase when the electron density is small, thereby increasing the total computer time.

D. Coulomb cross section and energy exchange

The Coulomb cross section and energy exchange during an *e-e* collision depend on the vector velocities of the projectile and target electrons. Since the method described here is effectively a PM technique, we have lost the vector information of the target electron. We approximated the interaction speed of the collisions as being the maximum of the speed of target and projectile. With this approximation for the interaction speed, we used the classical Coulomb cross section[25]

$$\sigma(v) = 4\pi b_0^2 \left[1 + \ln \left[\frac{\lambda_D}{b_0} \right]^2 \right]^{1/2}, \quad b_0 = \frac{e^2/4\pi\varepsilon_0}{\mu v^2}, \quad (7)$$

where μ is the reduced mass. Assuming isotropic scattering with angle $\theta = 2\cos^{-1}(r)$, the energy loss (positive) or energy gain (negative) for the projectile electron i scattering from the electron fluid element having energy ε_j was approximated as

$$\Delta\varepsilon_i = \begin{cases} \varepsilon_i[1+\cos(\theta)]/2, & \varepsilon_i > \varepsilon_j \\ -\varepsilon_j[1+\cos(\theta)]/2, & \varepsilon_i < \varepsilon_j \ . \end{cases} \qquad (8)$$

The change in energy is imparted to the projectile electron. The energy imparted to the target electron is implicitly accounted for when the EED is sampled during the next update of the probability arrays.

IV. RESULTS FOR MONTE CARLO SIMULATIONS WITH ELECTRON-ELECTRON COLLISIONS

In this section, we present results for the electron-energy distribution for swarms in N_2 and Ar under conditions where e-e collisions are important. In the first part of this section we have used a spatially uniform, time-invariant electric field. This allows us to make comparisons with the EED obtained by solving Boltzmann's equation using conventional continuum techniques. The method of solving Boltzmann's equation for this comparison is functionally equivalent to that used by Rockwood.[26] We then show EED's for spatially dependent and time-varying fields as a demonstration of the method.

The electron-energy distribution obtained with our MCS for electron swarms in Ar and N_2 are shown in Fig. 2. The applied field is $E/N = 20$ Td (1 Td $= 10^{-17}$ V cm^2). The electron-impact cross sections were obtained from Refs. 27 and 28 for Ar, and Refs. 28 and 29 for N_2. Elastic collisions with Ar$^+$ and N_2^+ and dissociative recombination collisions of electrons with N_2^+ were also included, although no collisions with excited states of Ar or N_2 were accounted for. Two cases are shown: excluding e-e collisions and including e-e collisions with a fractional ionization of $\delta = n_e/N = 5 \times 10^{-4}$. The EED's for the same conditions obtained from the continuum solution of Boltzmann's equation are also shown. Looking first at the results for Ar, the EED for $\delta = 0$ shows the typical cutoff at $\varepsilon \simeq 11$ eV resulting from the energy loss from electronic excitation of Ar. The EED with $\delta = 5 \times 10^{-4}$ appears more Maxwellian (which would be a straight line in the figure) due to the dominance of the energy exchange collisions between electrons. The EED is depressed at intermediate energies and enhanced at low and high energies compared to the case without e-e collisions. The EED's calculated using the MC method agree well with the continuum solutions. The EED's in N_2 show the cutoff at $\varepsilon \simeq 2$ eV resulting from vibrational excitation.

Electron-impact-rate coefficients for processes which have high-energy thresholds are quite sensitive to the fractional ionization. This results from the energy exchange during e-e collisions which repopulate the "tail" of the distribution which is depleted by inelastic collisions. For example, rate coefficients for electron-impact excitation and ionization, as computed with the MCS as a
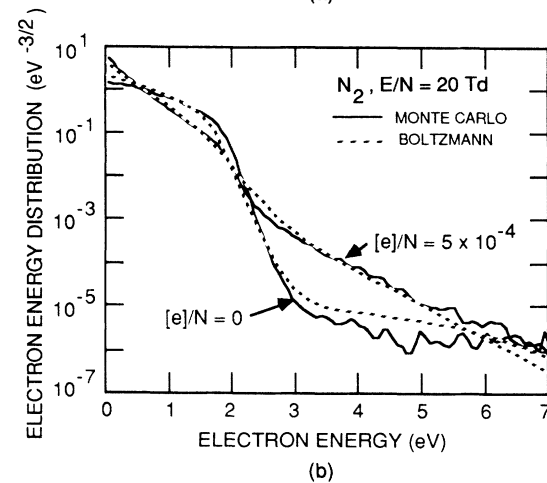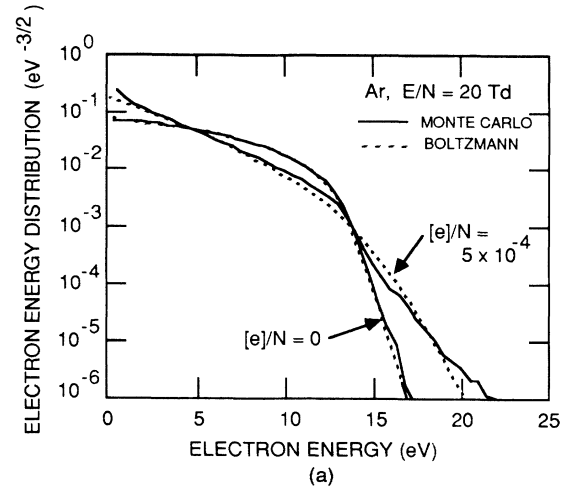

FIG. 2. Electron-energy distributions (EED's) for (a) Ar and (b) N_2 computed with Monte Carlo simulations (MCS) with and without e-e collisions. The fractional ionizations are $[e]/N = 0$ and 5×10^{-4}, respectively. The distributions are for $E/N = 20$ Td. The field is spatially and temporally uniform to enable comparison to EED's obtained by solving the continuum Boltzmann equation.

function of fractional ionization, are shown in Fig. 3, where they are also compared to rate coefficients obtained from the direct solution of Boltzmann's equation.[25] Processes having intermediate threshold energies such as excitation are not significantly effected by the raising of the tail of the EED, though the MCS show a somewhat stronger effect. Higher-threshold processes, such as ionization, are more acutely affected, with their rate coefficients increasing with increasing δ. The dependence of the rate coefficients on δ depend, of course, on the details of their cross sections. This dependence is shown in Fig. 4, where cross sections and rate coefficients for electron collisions with N_2 are shown as a function of δ. Rate coefficients for excitation of $N_2(v=1)$ and $N_2(v=8)$ decrease and increase, respectively, with increasing δ. The rate coefficient for electron-impact excitation of $N_2(A^3\Sigma)$ may, in fact, have a maximum as a
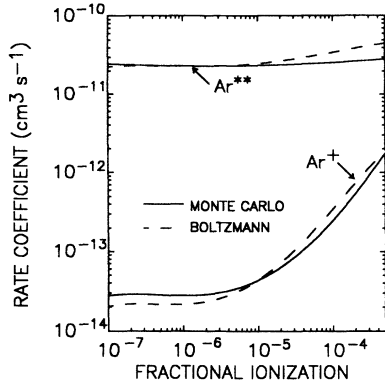
FIG. 3. Electron-impact-rate coefficients for Ar as a function of fractional ionization computed with the Monte Carlo simulation for $E/N = 20$ Td. The electric field is spatially and temporally uniform to enable comparison to rate coefficients obtained by solving the continuum Boltzmann equation.

function of δ due to the resonance nature of its cross section which is maximum at $\varepsilon = 11$ eV. As the frequency of electron-energy-exchange collisions increases, the density of low- and high-energy electrons increases at the expense of intermediate energies at which the cross section is
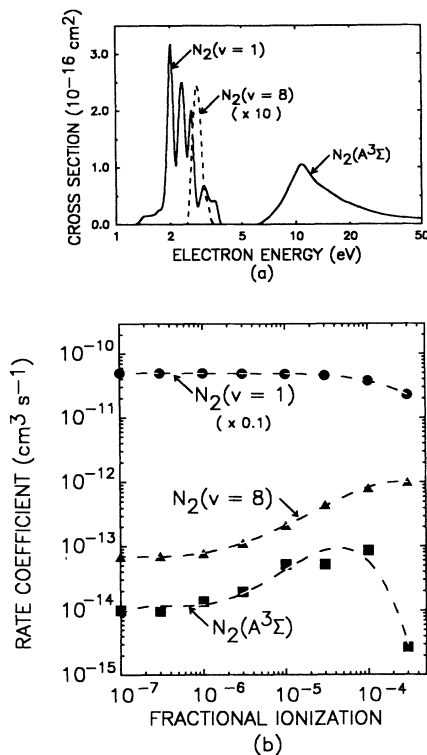
FIG. 4. Electron-impact cross sections (top) and rate coefficients for N_2 (bottom) as a function of fractional ionization computed with the Monte Carlo simulation for $E/N = 20$ Td. These results show that the behavior of rate coefficients on fractional ionization depends upon the details of their cross sections.

maximum. The coefficient therefore first experiences a shallow maximum as the tail of the distribution is lifted, and then decreases as more electrons appear at low energy when the EED thermalizes.

In low-pressure electric discharges where losses are dominated by diffusion, the electron density is usually maximum on the axis and lowest near the walls. Electron-impact-rate coefficients for high-threshold processes should then be higher on the axis of the discharge, where δ is the highest, than near the walls. To demonstrate this effect we simulated an electric discharge in Ar sustained between two flat plates. The EED as a function of position for a discharge in Ar is shown in Fig. 5(a). The gas pressure is 3.1 Torr ($N = 10^{17}$ cm^{-3}) and $E/N = 20$ Td. The electron density and electron-impact-rate coefficients for these conditions as a function of position are shown in Fig. 5(b). The larger electron density on the axis is sufficient to thermalize the EED by
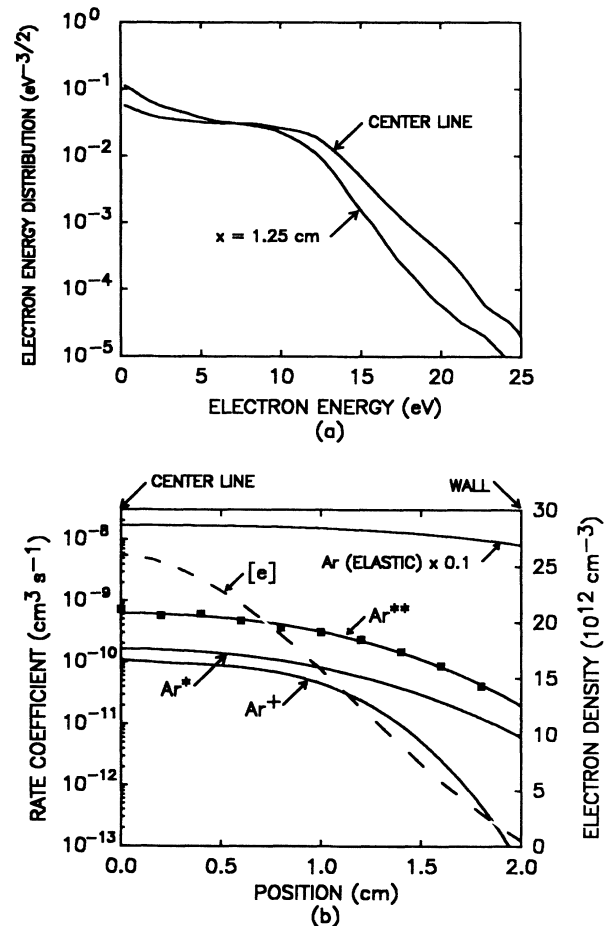

(a)

(b)

FIG. 5. Results from the MCS for a low-temperature partially ionized plasma sustained between two flat plates. The gas pressure is 3.1 Torr and the E/N is 20 Td. (a) Electron-energy distribution at the center line and 1.25 cm away from the axis. (b) Electron density [e] and electron-impact-rate coefficients as a function of position. The higher electron density on the axis of the discharge increases rate coefficients for high-threshold processes there, while lower threshold processes have rate coefficients which are more uniform as a function of position.

e-e collisions. The result is a significant increase in the electron-impact-rate coefficient for ionization near the axis compared to the wall. Lower-threshold processes (i.e., electronic excitation) and elastic collisions have rate coefficients which are more uniform as a function of position.

The temporal response of the EED to changes in the electric field is faster with e-e collisions than without those collisions. This effect is shown in Fig. 6, where the EED is plotted for an argon plasma. The applied electric field was decreased from 50 to 10 Td in 1 μs. The response of the EED to changes in E/N is faster with e-e collisions due to the higher rate of energy exchange between electrons which rapidly "communicates" the loss of energy due to inelastic collisions from one portion of the EED to another. The fractional rate of energy exchange for electrons below the inelastic threshold is limited to $2m_e/M$ per collision in the absence of e-e collisions. This rate is $2m_e/(M\delta)$ or 0.03 the rate in the presence of e-e collisions.

In magnetically assisted plasma processing reactors, such as ECR devices,[17–19] the fractional electron density can be $\leq 10^{-2}$, which is clearly in the regime where e-e collisions are important. Particle simulations of such de-

vices must therefore include e-e collisions for an accurate representation. This is particularly true of ECR devices where high values of δ not only change the value of rate coefficients in the manner discussed above, but may also affect the resonance condition. In ECR devices, a microwave electric field, at or near the electron cyclotron frequency, is applied to a magnetized plasma. Conventional ECR theory states that power deposition, and hence electron temperature, should scale as

$$P \approx \frac{n_e e^2 E}{2m_e v_m} \frac{1}{\left[1 + \left[\frac{\omega - \omega_c}{v_m}\right]^2\right]} .$$ (9)

In Eq. (9), v_m is the energy dissipation collision frequency, ω is the frequency of the applied electric field having amplitude E, and $\omega_c = eB/m_e$ is the electron cyclotron frequency for magnetic field B. As v_m increases, the width of the resonance increases, while the peak value decreases. This formulation is predicated on v_m being the frequency at which power is dissipated. In e-e collisions though, the net change in momentum and energy is zero, since the exchange is with another electron. One might expect then, that when δ is increased, the width of the resonance would increase by virtue of increasing the total collision frequency. The electron temperature, however, should not decrease proportionally, since the collision is not truly dissipative. To investigate this possibility, we simulated an ECR excited plasma with and without e-e collisions. The gas pressure was 50 mTorr of Ar and the microwave frequency at resonance was 1 GHz. The electron temperature ($\langle \varepsilon \rangle = \frac{3}{2}kT_e$) is plotted as a function of detuning of the magnetic field from resonance in Fig. 7. The electron temperature is slightly lower for $\Delta B = 0$ when including e-e collisions. The resonance, however, clearly has a greater width and sustains a higher temperature to large detuning.
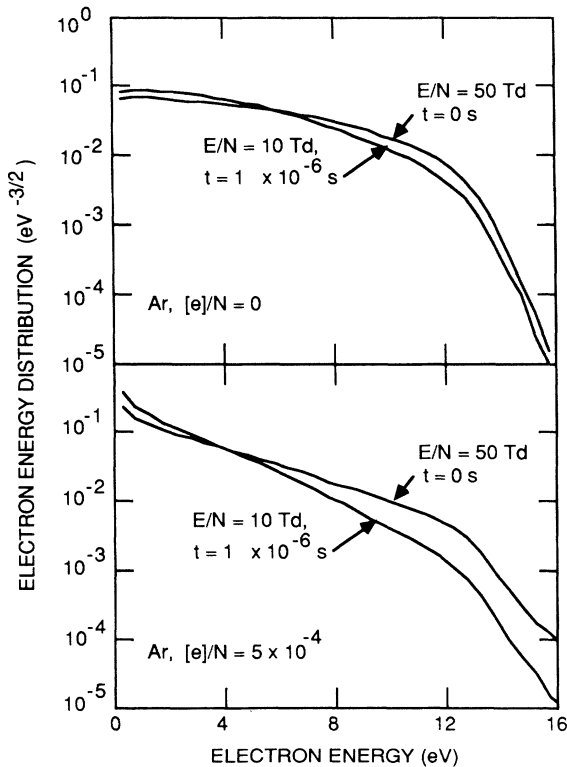
FIG. 6. Electron-energy distributions (EED's) as a function of time for electron swarms in argon in the absence (top) and presence (bottom) of electron-electron collisions. The fractional ionization is $[e]/N = 5 \times 10^{-4}$. The electric field was ramped from $E/N = 50$–10 Td in 1 μs. The response of the EED to changes in electric field is faster when including e-e collisions due to the rapid rate of energy exchange they afford.
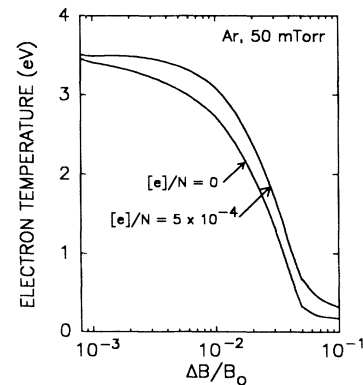
FIG. 7. Electron temperature ($\langle \varepsilon \rangle = \frac{2}{3}kT_e$) as a function of detuning of the magnetic field in an electron cyclotron resonance (ECR) plasma. The case including e-e collisions (fractional ionization $[e]/N = 5 \times 10^{-4}$) has a wider resonance.

V. CONCLUDING REMARKS

We have developed a method whereby electron-electron collisions may be included in a Monte Carlo simulation of the electron-energy distribution in partially ionized plasmas. This method is particularly appropriate when energy loss is dominated by inelastic collisions of electrons with neutral species and energy exchange is dominated by e-e collisions. The basis of the method is that e-e collisions are treated equivalently to electron–neutral-species collisions. The method is made tractable by using a modified null-cross-section technique. EED's calculated by the method compare well with the distribution function calculated using conventional solutions of Boltzmann's equation in a parameter space in which both are valid. The Monte Carlo technique described here has been shown to be applicable to multiple dimensions and to transients. The assumption of isotropic scattering during e-e collisions limits the application of this method as presented to plasmas having low average energies (a few to tens of electron volts) where only a minority of the collisions are forward scattered. The algorithm for the choice of scattering angle, though, can be easily replaced with one using an energy-resolved differential cross section with no other modifications to the model, but one must pay a minor penalty in an increase in computer time.

The utility of this method is in large part determined by practical considerations such as the amount of computer time required to implement it. We have experienced increases in computer time of a factor of 3–6 when including e-e algorithms compared to the same case without e-e collisions. This increase in computer time depends largely on the estimate of the amount of working null space that is required. Having excess null space increases the number of null collisions, and hence increases the computer time. A judicious choice in the amount of working null space required would result in the computer time being 2–3 times longer when using these algorithms compared to the conventional MCS without e-e collisions.

ACKNOWLEDGMENTS

[1]C. K. Birdsall and A. B. Langdon, *Plasma Physics via Computer Simulations* (McGraw-Hill, New York, 1985).

[2]R. W. Hockney and J. W. Eastwood, *Computer Simulations Using Particles* (McGraw-Hill, New York, 1981).

[3]J. M. Dawson, Rev. Mod. Phys. **55**, 403 (1983).

[4]J. W. Eastwood, Comput. Phys. Commun. **43**, 89 (1986).

[5]B. M. Penetrante, J. N. Bardsley, and L. C. Pitchford, J. Phys. D **18**, 1087 (1985).

[6]J. P. Boeuf and E. Marode, J. Phys. D **17**, 1133 (1984).

[7]G. Schaefer, G. F. Reinking, and K. H. Schoenbach, J. Appl. Phys. **61**, 120 (1987).

[8]K. Satoh, H. Itoh, Y. Nakao, and H. Tagashira, J. Phys. D **21**, 931 (1988).

[9]J. P. Boeuf and E. Marode, J. Phys. D **15**, 2169 (1982).

[10]S. Hashiguchi and M. Hasikuni, Jpn. J. Appl. Phys. **27,**, 1010 (1988).

[11]M. J. Kushner, Trans. Plasma Sci. **PS-14**, 188 (1985).

[12]T. J. Moratz, L. C. Pitchford, and J. N. Bardsley, J. Appl. Phys. **61**, 2146 (1987).

[13]R. W. Boswell and I. J. Morey, Appl. Phys. Lett. **52**, 21 (1988).

[14]M. J. Kushner, J. Appl. Phys. **61**, 2784 (1987).

[15]L. E. Kline, W. D. Partlow, and W. E. Bies, J. Appl. Phys. **65**, 70 (1989).

[16]M. Surrendra, D. B. Graves, and I. J. Morey, Appl. Phys. Lett. **56**, 1022 (1990).

[17]K. Shirai, T. Iizuka, and S. Gonda, Jpn. J. Appl. Phys. **28**, 897 (1989).

[18]Y. Lee, J. Heidenrich, and G. Fortuno, J. Vac. Sci. Technol. A **7**, 903 (1989).

[19]O. A. Popov, J. Vac. Sci. Technol. A **7**, 894 (1989).

[20]S. M. Rossnagle, J. Vac. Sci. Technol. A **6**, 1821 (1988).

[21]G. Y. Yeom, J. A. Thornton, and M. J. Kushner, J. Appl. Phys. **65**, 3816 (1989).

[22]S. Lin and J. N. Bardsley, J. Chem. Phys. **66**, 435 (1977).

[23]R. M. Yorston, J. Comp. Phys. **64**, 177 (1986).

[24]To minimize the number of null collisions during the simulation, the fraction of the probability array allocated to "working" null space should be kept as small as possible. In practice, this is complicated by the fact that the cross section for e-e collisions scales as $1/\varepsilon^2$ and therefore is largest at low energy. This results in a large fraction of null collisions at higher energy. This problem is avoided by dividing the energy range of interest into subranges. In each subrange the maximum electron-collision frequency is determined and a separate null-collision frequency is used in each subrange. Collision times and choices of collisions are then made based on which subrange the electron currently "resides." There is some ambiguity when an electron crosses from one subrange to an adjacent subrange during the flight between collisions, but the fraction of flights during which this occurs is small.

[25]M. Mitchner and C. H. Kruger, Jr., *Partially Ionized Gases* (Wiley, New York, 1973), pp. 54–62.

[26]S. D. Rockwood, J. Appl. Phys. **45**, 5229 (1974).

[27]K. Tachibana, Phys. Rev. A **34**, 1007 (1986).

[28]M. Hayashi, Nagoya Institute of Technology Report No. IPPJ-AM-19 (1981) (unpublished); D. Rapp and P. Englander-Golden, J. Chem. Phys. **43**, 1464 (1965).

[29]A. G. Engelhardt, A. V. Phelps, and C. G. Risk, Phys. Rev. **135**, A1566 (1964); A. V. Phelps and L. C. Pitchford, Phys. Rev. A **31**, 2932 (1985); G. J. Schulz, Phys. Rev. **135**, A988 (1964); D. Spence, J. L. Mauer, and G. J. Schulz, J. Chem. Phys. **57**, 5516 (1972); D. C. Cartwright, S. Trajmar, A. Chutjian, and W. Williams, Phys. Rev. A **16**, 1041 (1977); E. C. Zipf and R. W. McLaughlin, Planet. Space Sci. **26**, 449 (1978); W. L. Borst, Phys. Rev. A **5**, 648 (1972); R. T. Brinkman and S. Trajmar, Ann. Geophys. **26**, 201 (1972).